J. Nonlinear Funct. Anal. 2023 (2023) 29 https://doi.org/10.23952/jnfa.2023.29

MATHRES

Journal of Nonlinear Functional Analysis

Available online at http://jnfa.mathres.org

COMPARATIVE NUMERICAL STUDY OF INTEGRABLE AND NONINTEGRABLE DISCRETE MODELS OF NONLINEAR SCHRÖDINGER EQUATIONS

QIAN LUO[1], YAZHUO LI[1], HAOYU GUO[2], QUANDONG FENG[1,*]

[1]College of Science, Beijing Forestry University, Beijing 100083, China

[2]School of Information Science and Technology, Beijing Forestry University, Beijing 100083, China

Abstract. In this paper, we study efficiency of numerical simulation for integrable and nonintegrable discrete Nonlinear Schrödinger equations (NLSE). We first discretize the NLSE into two classical spatial models, nonintegrable direct discrete model and integrable Ablowitz-Ladik model. By some simple transformations and Doubarx transformation, we obtain two integrable models from Ablowitz-Ladik model. Then, five different kinds of schemes can be applied to simulate four models in bright and dark cases for comparing the performance in preserving the conserved quantities' approximations of NLSE. The numerical experiments indicate that Gauss symplectic method is more efficient than nonsymplectic schemes and splitting schemes when simulating the same model. Both intergrable models and nonintergrable model have their own advantages in preserving the conserved quantities' approximations. For the three integrable models, Ablowitz-Ladik Model and the model which has a general symplectic structure have similar simulation effects, and the model owing a cononical symplectic structure has low efficiency because the complicated Doubarx transformations make the model difficult to solve. Moreover, symplectic scheme and symmetric scheme have overwhelming superiorities over nonsymplectic schemes in preserving the invariants of Hamiltonian system.

Keywords. Ablowitz-Ladik model; Hamiltonian system; Nnonlinear Schrödinger equation; Nonintegrable; Symplectic scheme.

1. INTRODUCTION

The NLSE can be expressed as

$$\begin{cases} iu_t + u_{xx} + a|u|^2 = 0, \\ u(x,0) = u_0(x), \end{cases} \tag{1.1}$$

where $x \in \mathbb{R}$, a is a constant, and $u(x,t)$ is a complex function. It plays an important role in many physical areas, such as nonlinear optics, hydrodynamics, and plasma physics, and it is

*Corresponding author.

E-mail address: fengqd@bjfu.edu.cn (Q. Feng).

Received May 26, 2023; Accepted August 23, 2023.

a completely integrable system [6, 7, 12, 13, 14]. Different parameters and initial conditions lead to different solitons motion. For example, $|u_0(\pm\infty)| = 0$ with $a > 0$ induces bright solitons motion, while $|u_0(\pm\infty)| = \rho$ (non-zero constant) with $a < 0$ induces dark solitons motion. In this paper, the two cases of solitons motion are discussed.

Using the inverse scattering transform, we can give the solution of NLSE [24]. However, the analytical solutions are difficult to obtain except for the special initial conditions. For this reason, a large of numerical methods have been constructed to simulate the NLSE [3, 5, 9, 11, 13, 15, 16, 18, 22, 25]. Usually, these methods discretize the NLSE into ordinary differential equations of space variants. Unfortunately, not all these methods can obtain expected results, unphysical ”blow-up” and ”numerical chaos” may occur with unreasonable discretization. Possessing structure-preserving property and long-time tracking ability of the solitons motion, symplectic methods have been favored for simulating the NLSE recently. Before employing the symplectic methods, we need to discretize the NLSE spatially into ordinary differential equations. There are two classical spatial discrete models, one of which is called direct discrete model (represented by Model I):

$$i\frac{dU_l}{dt} + \frac{U_{l+1} - 2U_l + U_{l-1}}{h^2} + a|U_l|^2 U_l = 0, \tag{1.2}$$

where h is the spatial step-size and $U_l(t) = U(lh,t), l = \cdots, -1, 0, 1, \cdots$.

The other spatial discretization model is called Ablowitz-Ladik model (A-L model, represented by Model II) :

$$i\frac{dU_l}{dt} + \frac{U_{l+1} - 2U_l + U_{l-1}}{h^2} + \frac{a}{2}|U_l|^2 (U_{l-1} + U_{l+1}) = 0, \tag{1.3}$$

Model I can be represented as a canonical Hamiltonian system which has canonical symplectic structure. Thus symplectic methods can be employed for simulation. By using two symplectic numerical schemes, Tang et al. successfully simulated NLSE, and their numerical results demonstrated that symplectic methods behave better than nonsymplectic methods in long-time simulations and preservation of invariants [19]. Via explicit splitting technique, Guan et al. integrated the NLSE, and their numerical results indicated that the explicit symplectic scheme has better performance than the implicit one [8]. Here, we note that, although expected experimental results have been obtained, Model I is not integrable, which means it cannot inherit the integrable property of the original NLSE.

For Model II, it is completely integrable [1], and thus inherit the integrable property of the original NLSE. However, it is not a canonical Hamiltonian system. By scaling and isometric transformations, Model II can be represented as a general Hamiltonian system (represented by Model III). Via Darboux coordinate transformation, Model III can be transformed into a Hamiltonian system with canonical symplectic structure, and we represent the canonical Hamiltonian system as Model IV. Zhang et al. demonstrated that the numerical results obtained from Model III are very similar to those obtained from Model IV [26]. In addition, K-symplectic methods by using spitting technique were constructed, and are more efficient than symplectic methods [27, 28]. Other researchers also demonstrated the symplectic schemes’ superiorities over non-symplectic ones when simulating the NLSE [20, 21, 23].

For model IV, it has canonical symplectic structure, and also is integrable. It seems that Model IV is optimal choice. However Darboux coordinate transformation makes Model IV very complicate, which results in time-consuming simulation. Therefore, in the view of simulation efficiency, Model IV is not the optimal choice.

Up to now, there are few results on which model is more efficient when simulating the NLSE. Therefore, in this paper, we give a systematic comparison for the nonintegrable model and three integrable models, and obtain some conclusions about simulation efficiency.

The paper is organized as follows: in Section 2, we give the first five conserved quantities of the original NLSE, and then obtain approximations of the conserved quantities via central difference. In Section 3, we standardize the A-L model by scaling transformation, isometric transformation, and coordinate transformation. In Section 4, we construct a splitting K-symplectic methods for general Hamiltonian system in bright and dark cases. In Section 5, we list the numerical schemes employed in numerical simulation, including symplectic scheme, nonsymplectic scheme, symmetric scheme, nonsymmetric scheme, splitting scheme, and so on. In Section 6, we present all the numerical results and give a conclusion in the final section.

2. Conserved Quantities of NLSE and Their Approximations

The NLSE has an infinite number of conserved quantities, such as the momentum, the energe, the charge, and so on; see, e.g., [14, 24]. Here we present the first six ones $D_1,\cdots,D_5$ as follows:

$$D_1=\int_{-\infty}^{+\infty}(|U|^2-\rho^2)dx,\qquad D_2=\int_{-\infty}^{+\infty}\{U\overline{U}_x-\overline{U}U_x\}dx,$$

$$D_3=\int_{-\infty}^{+\infty}\{2|U_x|^2-a(|U|^4-\rho^4)\}dx,\qquad D_4=\int_{-\infty}^{+\infty}\{2\overline{U}_xU_{xx}-3a|U|^2\overline{U}U_x\}dx,$$

$$D_5=\int_{-\infty}^{+\infty}\{2|U_{xx}|^2-6a|U|^2|U_x|^2-a((|U|^2)_x)^2+a^2(|U|^6-\rho^6)\}dx,$$

where $\overline{U}$ is the complex conjugation of U. It should be noted that the conserved quantities above-mentioned are in the case of dark soliton; if ρ is removed, they present the conserved quantities of bright soliton. Utilizing central different

$$U_x(lh,t)=\frac{U_{l+1}-U_{l-1}}{2h},$$

$$U_{xx}(lh,t)=\frac{U_{l+1}-2U_l+U_{l-1}}{h^2},$$

$$U_{xxx}(lh,t)=\frac{U_{l+2}-2U_{l+1}+2U_{l-1}-U_{l-2}}{2h^3},$$

we can give the approximation to conserved quantities $D_1,\cdots,D_5$ with error $O(h^2)$ or $O(h^4)$:

$$F_1=h\sum_l(U_l\overline{U}_l-\rho^2),$$

$$F_2=\sum_l\{U_l\overline{U}_{l+1}-U_{l+1}\overline{U}_l\},$$

$$F_3=\frac{1}{2h}\sum_l\{2|U_l|^2-U_{l+1}\overline{U}_{l-1}-U_{l-1}\overline{U}_{l+1}\}-ah\sum_l(|U_l|^4-\rho^4),$$

$$\cdots\cdots$$

We denote $F_m=FR_m+iFI_m, m=1,2,3$, where FR_m and FI_m are the real part and imaginary part of F_m, respectively. After calculation, we obtain that FI_1, FR_2, and FI_3 are equal to zero.

Therefore, the preservation of the left three approximations will be used as an indicator of simulation precision in numerical experiments section.

3. A-L Model's Standardization by Doubarx Transformation

For bright solitons, by the scaling transformation $V_l = \sqrt{\frac{ah^2}{2}}U_l, a > 0, l = \cdots, -1, 0, 1, \cdots;$ $s = -\frac{t}{h^2}$, A-L Model (also denoted by Model II) can be written as

$$i\frac{dV_l}{ds} = V_{l+1} - 2V_l + V_{l-1} + |V_l|^2(V_{l+1} + V_{l-1}), \tag{3.1}$$

Similarly, for dark solitons motion, by $V_l = \sqrt{\frac{-ah^2}{2}}U_l, a < 0$, A-L Model can be written as

$$i\frac{dV_l}{ds} = V_{l+1} - 2V_l + V_{l-1} - |V_l|^2(V_{l+1} + V_{l-1}). \tag{3.2}$$

By using isometric transformation $X_l = V_l exp(-2si)$ and denoting $X_l = p_l + iq_l, l = \cdots, -1, 0, 1, \cdots,$ we can rewrite equation (3.1) and (3.2) respectively, as follows:

$$i\frac{dX_l}{ds} = (1 + |X_l|^2)(X_{l+1} + X_{l-1}) \tag{3.3}$$

and

$$i\frac{dX_l}{ds} = (1 - |X_l|^2)(X_{l+1} + X_{l-1}). \tag{3.4}$$

For convenience, we denote (3.3) and (3.4) as Model III, which both can be expressed as the general Hamiltonian system

$$\frac{d}{ds}Z = K^{-1}(Z)\nabla H(Z), \tag{3.5}$$

where $Z = [p^T, q^T]^T$, and $p = [p_{-n}, \cdots, p_n]^T, q = [q_{-n}, \cdots, q_n]^T$,

$$K^{-1}(Z) = (k_{ij}(Z))_{(4n+2)\times(4n+2)} = \begin{bmatrix} O_{2n+1} & D \\ -D & O_{2n+1} \end{bmatrix},$$

$D = diag\{W_{-n}, \cdots, W_n\}, O_{2n+1}$ is $(2n+1)\times(2n+1)$ null matrix. $W_l = 1 + p_l^2 + q_l^2, l = \cdots, -1, 0, 1, \cdots$ for the bright solitons motion, and $W_l = 1 - p_l^2 - q_l^2, l = \cdots, -1, 0, 1, \cdots$ for the dark solitons motion. The Hamiltonian is

$$H(Z) = \sum_{l=-n}^{n}\big(p_l p_{l+1} + q_l q_{l+1}\big),\ for\ bright\ solitons\ motion,$$

$$H(Z) = \sum_{l=-n}^{n}\left(p_l p_{l+1} + q_l q_{l+1} + \frac{a}{2}h^2\rho^2\right),\ for\ dark\ solitons\ motion. \tag{3.6}$$

By Doubarx transformations [2, 4] $\varphi : \mathbb{R}^{4n+2} \to \mathbb{R}^{4n+2}, \varphi(Y) = Z$, any general Hamiltonian system of form (3.5) can be standardized. Here, we give two different doubarx transformations:

For bright solitons motion:

$$\begin{cases} p_l = \sqrt{1+u_l^2}tan\left(\sqrt{1+u_l^2}v_l\right), \\ q_l = u_l, \end{cases}$$

with inverse

$$\begin{cases} u_l = q_l, \\ v_l = \dfrac{arctan\left(\dfrac{p_l}{\sqrt{1+q_l^2}}\right)}{\sqrt{1+q_l^2}}, \end{cases}$$

and correspongding canonical Hamiltonian

$$G(u,v) = \sum_l \Big\{ u_l u_{l+1} + \sqrt{1+u_l^2}\sqrt{1+u_{l+1}^2}$$
$$tan\big(\sqrt{1+u_l^2}v_l\big)tan\big(\sqrt{1+u_{l+1}^2}v_{l+1}\big)\Big\}.$$

For dark solitons motion:

$$\begin{cases} p_l = \sqrt{\dfrac{1-exp\left\{-(u_l^2+v_l^2)\right\}}{u_l^2+v_l^2}}v_l, \\ q_l = \sqrt{\dfrac{1-exp\left\{-(u_l^2+v_l^2)\right\}}{u_l^2+v_l^2}}u_l, \end{cases}$$

with inverse

$$\begin{cases} u_l = \sqrt{-\dfrac{ln(1-p_l^2-q_l^2)}{p_l^2+q_l^2}}q_l, \\ v_l = \sqrt{-\dfrac{ln(1-p_l^2-q_l^2)}{p_l^2+q_l^2}}p_l, \end{cases}$$

and corresponding canonical Hamiltonian

$$G(u,v) = \sum_{l=-n}^{n} \Bigg\{ \sqrt{\frac{1-exp\left\{-(u_l^2+v_l^2)\right\}}{u_l^2+v_l^2}} \sqrt{\frac{1-exp\left\{-(u_{l+1}^2+v_{l+1}^2)\right\}}{u_{l+1}^2+v_{l+1}^2}}$$
$$(u_l u_{l+1} + v_l v_{l+1}) + \frac{a}{2}h^2\rho^2 \Bigg\}$$

Then (3.3) and (3.4) can be represented as a canonical Hamiltonian system (denoted by Model IV) $\frac{d}{ds}Y = J^{-1}\nabla G(Y)$ with $G(Y) = H \circ \varphi(Y)$, where $Y = [u^T, v^T]^T, u = [u_{-n}, \cdots, u_n]^T, v = [v_{-n}, \cdots, v_n]^T, J = \begin{bmatrix} O_{2n+1} & I_{2n+1} \\ -I_{2n+1} & O_{2n+1} \end{bmatrix}$, and I_{2n+1} is $(2n+1)\times(2n+1)$ identity matrix.

4. Splitting K-symplectic Methods for Model III

The general Hamiltonian system (3.5) with Hamiltonian $H(z) = H_1(p) + H_2(q)$ and $K^{-1}(z) = \begin{bmatrix} O_{2n+1} & -K_{12}(p,q) \\ K_{12}^T(p,q) & O_{2n+1} \end{bmatrix}$ can be decomposed into two subsystems as

$$\begin{cases} \dot{p} = 0, \\ \dot{q} = K_{12}(p,q)^T \nabla_p H_1(p), \end{cases} \tag{4.1}$$

and

$$\begin{cases} \dot{p} = -K_{12}(p,q)\nabla_q H_2(q), \\ \dot{q} = 0. \end{cases} \tag{4.2}$$

If these two subsystems can be solved explicitly, we can construct K-symplectic methods by composing analytical solutions of the corresponding subsystems. We denote the analytical solutions of (4.1) and (4.2) by ψ_1^t and ψ_2^t, and then splitting method $\psi_1^t \circ \psi_2^t$ is K-symplectic with one-order, and $\psi_1^{\frac{t}{2}} \circ \psi_2^t \circ \psi_1^{\frac{t}{2}}$ is K-symplectic with second-order [17].

In dark solitons case, general Hamiltonian function (3.6) can be separated into $H_1 = \sum_{-\infty}^{\infty}(p_l p_{l+1})$ and $H_2 = \sum_{-\infty}^{\infty}(q_l q_{l+1} + \frac{a}{2}h^2\rho^2)$. Then we can solve the two subsystems exactly, the corresponding analytical solutions are

$$\psi_1^t : \begin{cases} p_i(t) = p_i, \\ q_i(t) = \dfrac{C_1 e^{M_1 t} - 1}{C_1 e^{M_1 t} + 1} \cdot \sqrt{1 - p_i^2}, \end{cases}$$

$$\psi_2^t : \begin{cases} p_i(t) = \dfrac{C_2 e^{M_2 t} - 1}{C_1 e^{M_2 t} + 1} \cdot \sqrt{1 - q_i^2}, \\ q_i(t) = q_i, \end{cases}$$

where

$$\begin{cases} C_1 = \dfrac{\sqrt{1-p_i^2} + q_i}{\sqrt{1-p_i^2} - q_i}, M_1 = -2(p_{i+1} + p_{i-1})\sqrt{1-p_i^2}, \\ C_2 = \dfrac{\sqrt{1-q_i^2} + p_i}{\sqrt{1-q_i^2} - p_i}, M_2 = -2(q_{i+1} + q_{i-1})\sqrt{1-q_i^2}, \end{cases}$$

$i = \cdots, -1, 0, 1, \cdots$, and p_i, q_i are the initial value. By similar technique, we can also derive the subsystems' solutions in bright solitons case as follows:

$$\phi_1^t : \begin{cases} \tilde{p}_i(t) = p_i, \\ \tilde{q}_i(t) = \dfrac{C_1 - tan(M_1 t)}{C_1 + tan(M_1 t)}, \end{cases}$$

and

$$\phi_2^t : \begin{cases} \tilde{p}_i(t) = \dfrac{C_2 + tan(M_2 t)}{C_2 - tan(M_2 t)}, \\ \tilde{q}_i(t) = q_i, \end{cases}$$

where

$$\begin{cases} C_1 = \dfrac{q_i}{1+p_i^2}, M_1 = \sqrt{1+p_i^2}(p_{i+1} + p_{i-1}), \\ C_2 = \dfrac{p_i}{1+q_i^2}, M_1 = \sqrt{1+q_i^2}(q_{i+1} + q_{i-1}). \end{cases}$$

Then we can employ directly the second-order Strang's splitting method

$$\Phi_2 \equiv \phi_1^{\frac{t}{2}} \circ \phi_2^t \circ \phi_1^{\frac{t}{2}},\ for\ bright\ solitons\ motion,$$

$$\Psi_2 \equiv \psi_1^{\frac{t}{2}} \circ \psi_2^t \circ \psi_1^{\frac{t}{2}},\ for\ dark\ solitons\ motion.$$

to simulate Model III.

5. Numerical Schemes

In this section, several different numerical schemes are presented, including symplectic scheme, symmetric scheme, nonsymplectic and nonsymmetric scheme, splitting schemes, etc.

Symplectic-symmetric Scheme (S1): Midpoint rule

$$Z_{n+1} = Z_n + \tau f\left(\frac{Z_{n+1} + Z_n}{2}\right).$$

The scheme is actually a Gauss method. It is symmetric in τ, and symplectic with second-order for canonical Hamiltonian systems.

Nonsymplectic-nonsymmetric R-K Shceme (S2):

$$\begin{cases} Z_{n+1} = Z_n + \frac{\tau}{4}[f(R_1) + 3f(R_2)], \\ R_1 = Z_n + \frac{\tau}{3}[f(R_1) - f(R_2)], \\ R_2 = Z_n + \frac{\tau}{9}[(2+2\sqrt{3})f(R_1) + 3f(R_2)]. \end{cases}$$

The scheme is nonsymmetric in τ with second-order, and nonsymplectic for canonical Hamiltonian systems.

Symplectic-symmetric Scheme (S3): the L-L-N splitting method

$$Z_{n+1} = \Phi^t(Z_n) = \phi_1^{\frac{\tau}{2}} \circ \phi_2^{\frac{\tau}{2}} \circ \phi_3^{\tau} \circ \phi_2^{\frac{\tau}{2}} \circ \phi_1^{\frac{\tau}{2}}(Z_n).$$

For Model I, the Hamiltonian system can be decomposed into $H_1 + H_2 + H_3$. We can easily obtain the solutions for the three subsystems. Similar to Section 4, we can obtain a symplectic and symmetric splitting method with second-order. One can refers to [8] for more details.

Symplectic -symmetric Scheme (S4): the Strang's splitting method

$$Z_{n+1} = \Psi^t(Z_n) = \psi_1^{\frac{\tau}{2}} \circ \psi_2^t \circ \psi_1^{\frac{\tau}{2}}(Z_n).$$

The scheme is K-symplectic for Model III with second-order.

Nonsymplectic-symmetric R-K Scheme (S5):

$$\begin{cases} Z_{n+1} = Z_n + \frac{\tau}{2}[f(R_1) + f(R_2)], \\ R_1 = Z_n + \frac{\tau}{12}[2f(R_1) + 3f(R_2)], \\ R_2 = Z_n + \frac{\tau}{12}[3f(R_1) + 4f(R_2)]. \end{cases}$$

The scheme is symmetric in τ with second-order, but nonsymplectic for canonical Hamiltonian systems.

We use the above five different schemes to simulate bright solitons and dark solitons respectively, and test the time evolutions of the conserved quantities' approximations of NLSE. These five schemes are all second-order. Moreover S3 and S4 are explicit, S3 can be employed in Model I (canonical Hamiltonian system), and S4 can be used in Model III (general Hamiltonian system).

6. Numerical Experiments

In this section, four different models, namely Model I (the direct discrete model), Model II (the untransformed A-L model), Model III (the A-L model after scaling and isometric transformation), and Model IV (the standardized A-L model). As mentioned above, Model I and Model IV are the canonical Hamiltonian systems, and Model III is the generalized Hamiltonian system.

6.1. **Initial conditions.** We give the initial conditions of the bright solitons in the following:

$$u(x,0) = 2\eta\sqrt{\frac{2}{a}}e^{2\chi x i} sech[2\eta(x-x_1)],$$

where $a=2, \eta=0.5, \chi=0.5$, and $x_1=0.0$. For the dark solitons, the initial conditions are :

$$u(x,0) = \rho\frac{1+e^{i2\theta}e^{\lambda(x-x_0)}}{1+e^{\lambda(x-x_0)}},$$

where $a=-2, \lambda=\sqrt{-2a}\rho sin\theta, \rho=0.72, \theta=0.75$, and $x_0=0.0$.

We simulate the four models in bright and dark solitons motion with spatial inteval $x \in [-900,900]$ and temporal interval $t \in [0,100]$. We choose six different sets of spatial step-size h and temporal step-size τ as follows :

	1	2	3	4	5	6
h	0.6	0.5	0.4	0.3	0.2	0.15
τ	0.04	0.025	0.02	0.01	0.005	0.0025

As it is difficult to obtain the analytical solution of the original NLSE with general conditions, we use the error of the conserved quantities' approximations FR_1, FI_2, FR_3 as an indicator of simulation accuracy, which is a traditional choice in numerical simulation field [8, 19, 20, 21, 23, 26, 27, 28]. For each scheme in our numerical experiments, we compare the accuracy of the conserved quantities' approximations (for different spatial step-size and temporal step-size) as a function of the CPU simulation time. Then we get the efficient figures of numerical schemes.

6.2. **Different schemes for same model.** In this sub-section, we apply different schemes to same model in order to show which scheme is more efficient. For simplicity, we call $err(A) = A(t)-A(0)$ for any variable A, and $max|err(A)|$ expresses the maximum absolute error of variable A. In the following, we discuss it in bright and dark solitons motion, and present numerical results with schemes S1, S2, S3 for Model I, and S1, S2, S4 for Model III (different applied splitting methods S3, S4 because of different models' function structures). Model I is a canonical Hamiltonian system, so Gauss symplectic methods applied to the system have overwhelming superiorities over nonsymplectic ones in long-time simulation and preservation of invariants. Model III is a general Hamiltonian system, Gauss symplectic method and K-symplectic scheme also should have similar superiorities over nonsymplectic ones in theory. The experimental results are displayed in the Figure 1 and Figure 2, respectively.

In bright solitons case, from Figure 1, we find S1 behaves better than S2, S3, S4, especially in (a) and (c). It means the second Gauss symplectic method is significantly efficient than nonsymplectic-nonsymmetric scheme S2, also than the explicit symplectic scheme S3 and S4. Although splitting method S3 and S4 are symplectic or K-symplectic, and can be implemented easily, it doesn't show high efficiency over nonsymplectic-nonsymmetric scheme S2 with same order, which is unexpected.

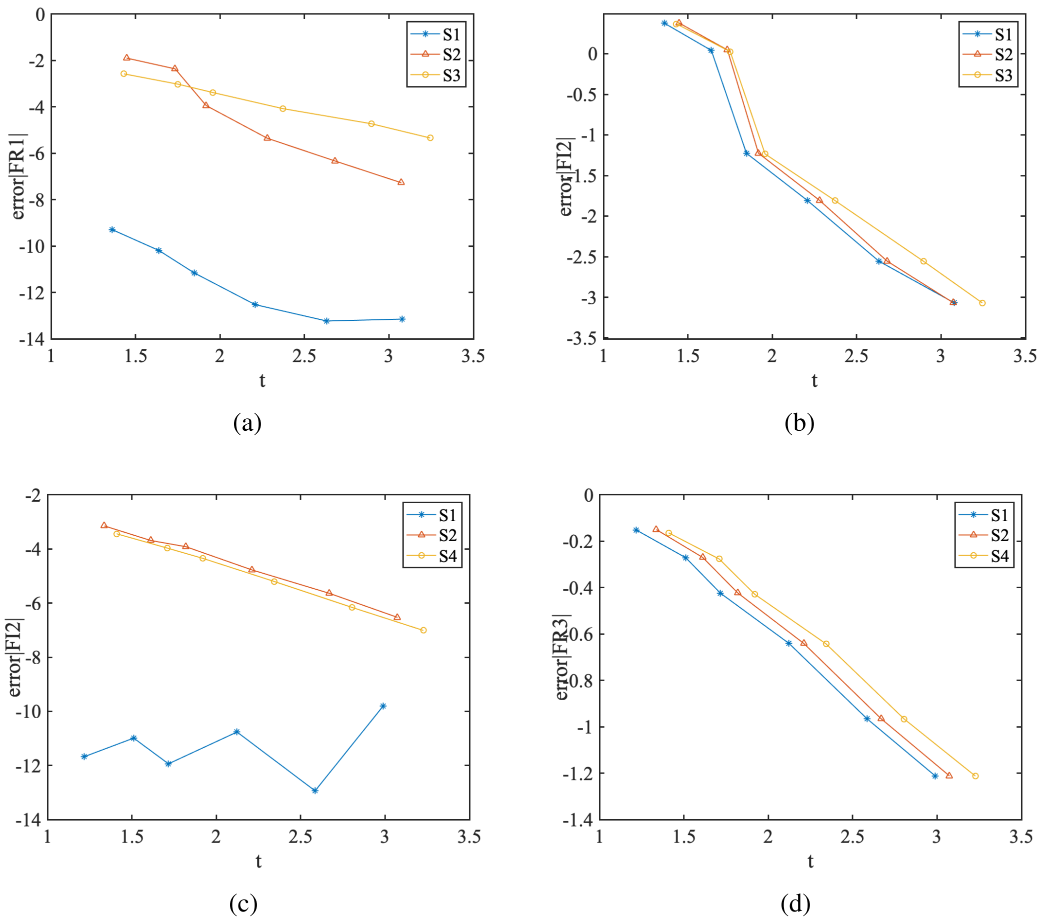

FIGURE 1. (a), (b): conserved quantities' approximations FR_1, FR_3's errors of S1,S2 and S3 versus CPU times of Model in bright solitons motion; (c), (d): conserved quantities' approximations FI_2, FR_3's errors of S1,S2 and S4 versus CPU times of Model III in bright solitons motion.

In dark solitons case, from Figure 2, we also find S1 behaves better than S2, S3, and S4, especially in (a) and (c). It is similar to bright solitons case. In addition, symplectic scheme S3 behaves better than nonsymplectic-nonsymmetric scheme S2 in (a) and (b) of Figure 2, the essential reason is that Model I is canonical Hamiltonian system.

The above result demonstrates that Gauss symplectic methods have overwhelming superiorities over nonsymplectic scheme and explicit symplectic scheme (splitting method). Moreover, it seems that explicit symplectic scheme do not take the advantage of comsuming less time and

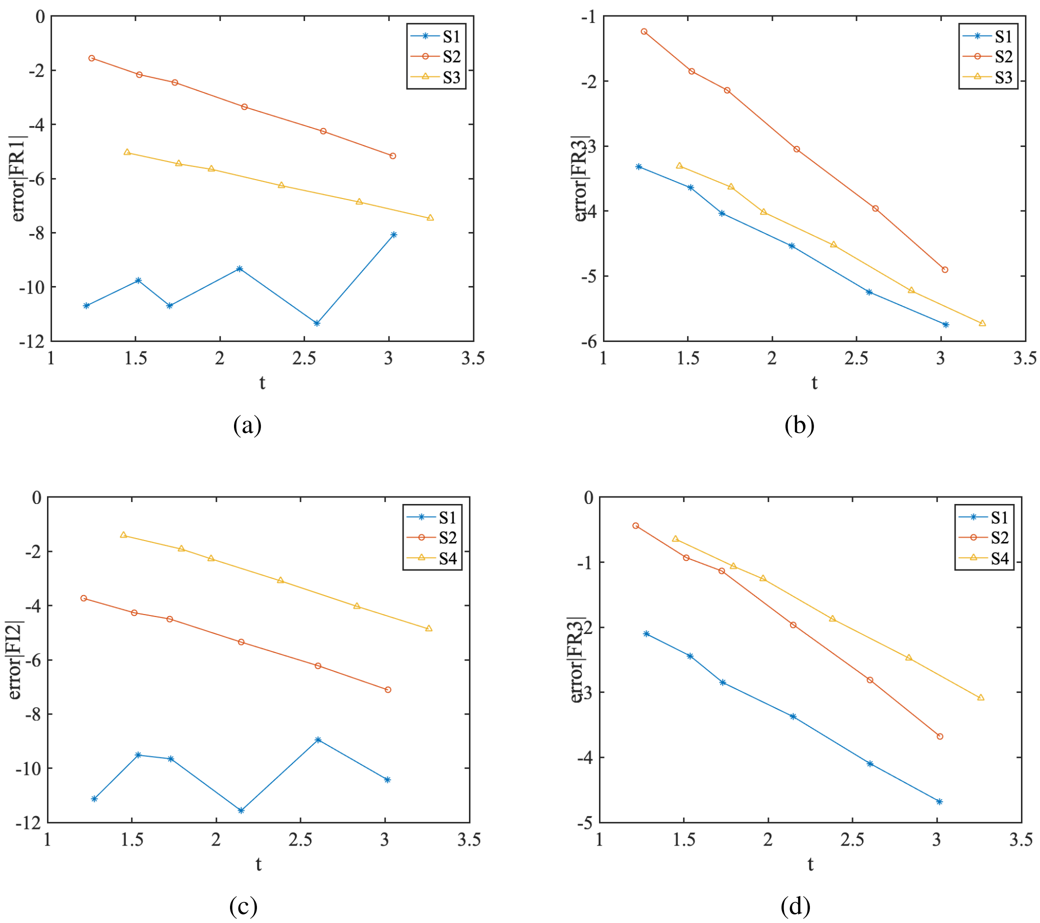

FIGURE 2. (a), (b): conserved quantities' approximations FR_1, FI_2's errors of S1,S2 and S3 versus CPU times of Model I in dark solitons motion; (c), (d): conserved quantities' approximations FI_2, FR_3's errors of S1,S2 and S4 versus CPU times of Model III in dark solitons motion.

possessing symplectic structure when simulating Model III, the most possible reason is that Model III is not a canonical Hamiltonian system.

6.3. **Same scheme for different models.** Different models have different properties, which lead to different numerical simulation effects. In this sub-section, we compare the simulation performance of different models with same scheme in preserving the conserved quantities' approximations.

For the Model I, namely direct discretization model, it is a canonical Hamiltonian system, but nonintegrable. For the Model II (A-L model), it is integrable, but not a Hamiltonian system. After some simple scaling and isometric transformations, Model II can be transformed into Model III. For Model III, it is a general Hamiltonian system, and also integrable. Applying complicated Doubarx transformations to the Model III, we can obtain the Model IV, which is a integrable and canonical Hamiltonian system.

Gauss methods are A-stable, B-stable, and have superiorities in long-time simulation, so we employ the first selected Gauss method with order two, that is the midpoint scheme S1, to simulate different models. From Figure 3. it is obvious that for the different conserved quantities' approximations FR_1, FI_2, and FR_3, the integrable and nonintegarable models play different advantages. For FR_1, we can clearly see that the results obtained in Model I is significantly more efficient than those of the other three models in (a) and (b) of Figure 3. The main reason is that FR_1 is the quadratic invariant of Model I which is a canonical Hamiltonian system , and Gauss symplectic method S1 can exactly preserve all the quadratic invariants. For FI_2 in (c) and (d), the integrable systems of Model II, III, and IV behave better than the nonintegrable Model I. For FR_3 in (e) and (f), in the case of bright solitons motion, the results obtained in three integrable models are more efficient than the nonintegrable Model I, while the results are just the reverse in the case of dark solitons motion.

As a whole, for the integrable models, the results obtained from Model II and Model III are very similar, mainly because Model III is transformed from Model II by some simple transformations. Model IV is a canonical Hamiltonian system, and also integrable. It seems that the Model IV should be the best in integrable models, however it behaves worst. It is not surprising at all. The reason is that Model IV is obtained from Model III by Doubarx transformations which are complicated. It makes implementation very time-consuming and leads to inefficiency.

6.4. **Symplectic and symmetric schemes compared with nonsymplectic-nonsymmetric sch emes in a canonical Hamiltonian system.** We note that the indicator of simulation accuracy used is the error of the conserved quantities' approximations FR_1, FI_2, FR_3 in sub-section 6.2 and 6.3, however these approximations are obtained by discretizing the conserved quantities of the original Schrodinger equation, usually are not the invariants of Hamiltonian systems. Therefore the symplectic methods can not fully show its advantages, especially for explicit symplectic scheme S3 in (a), (b) of Fig. 1. If we apply symplectic schemes to a canonical Hamiltonian system, and use the error of Hamiltonian systems' invariants as an indicator of simulation accuracy, symplectic schemes' advantages will be showed fully.

In this sub-section, the performance of symplectic scheme and symmetric scheme will be compared with nonsymplectic-nonsymmetric scheme in a canonical Hamiltonian system. We choose scheme S1, S2, S5, which represent the symplectic scheme, nonsymplectic-nonsymmetric scheme and symmetric scheme, respectively, and choose Model I, which represent the canonical Hamiltonian system. The energy E and charge Q are the two invariants of Model I (for more details, see [19]), then we use the error of these two invariants as an indicator of simulation accuracy.

From Figure 4, the symplectic scheme S1 has obvious advantage over the nonsymplectic-nonsymmetric scheme S2, especially in (b), (c), and (d). Meanwhile, we can find the performance of symmetric schemes is very similar to that of symplectic schemes in most cases, especially in the case of dark solitons motion. The main reason is that symmetric schemes are very closely related to symplectic schemes, if linear problems and other conditions are satisfied, symmetric Runge–Kutta schemes will be equivalent to the symplectic schemes [10]. From above experimental results, symplectic schemes and symmetric schemes have overwhelming superiorities over the nonsymplectic-nonsymmetric scheme in long-time preserving invariants of the original Hamiltonian.

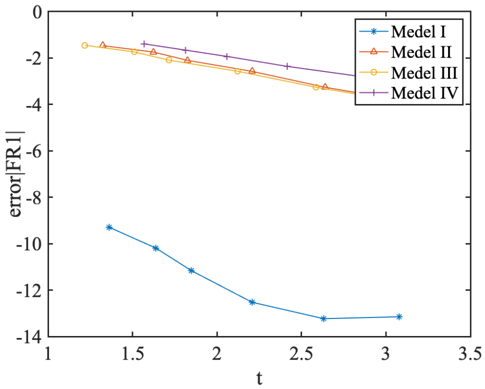

(a)

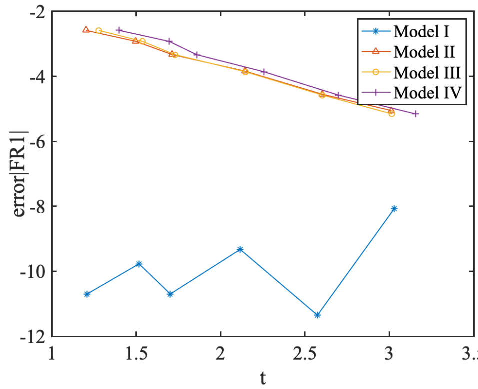

(b)

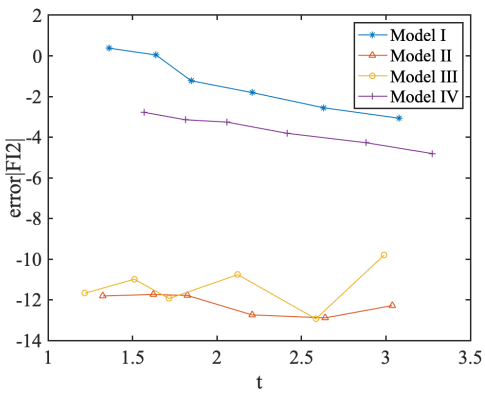

(c)

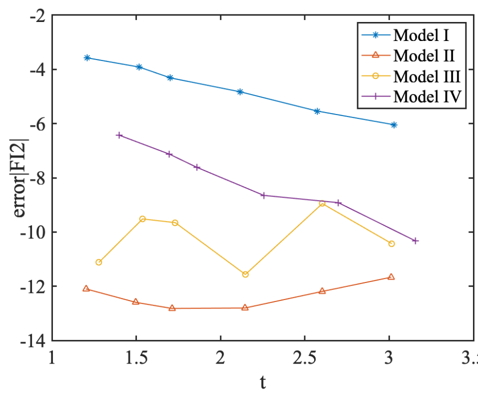

(d)

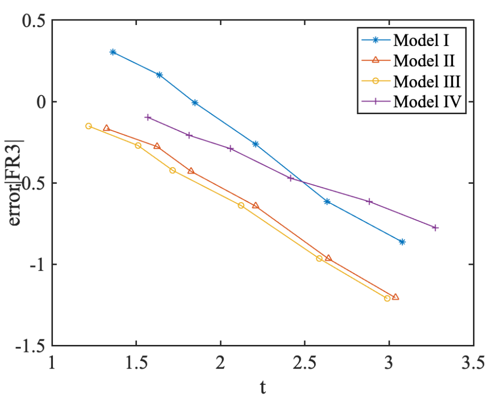

(e)

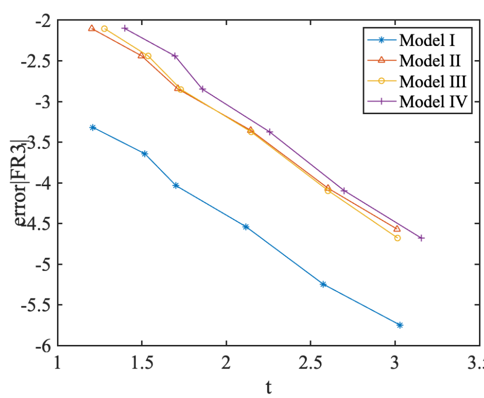

(f)

FIGURE 3. (a), (c), (e): conserved quantities' approximations FR_1, FI_2, FR_3's errors versus CPU times in bright solitons case; (b), (d), (f): conserved quantities' approximations FR_1, FI_2, FR_3's errors versus CPU times in dark solitons case.

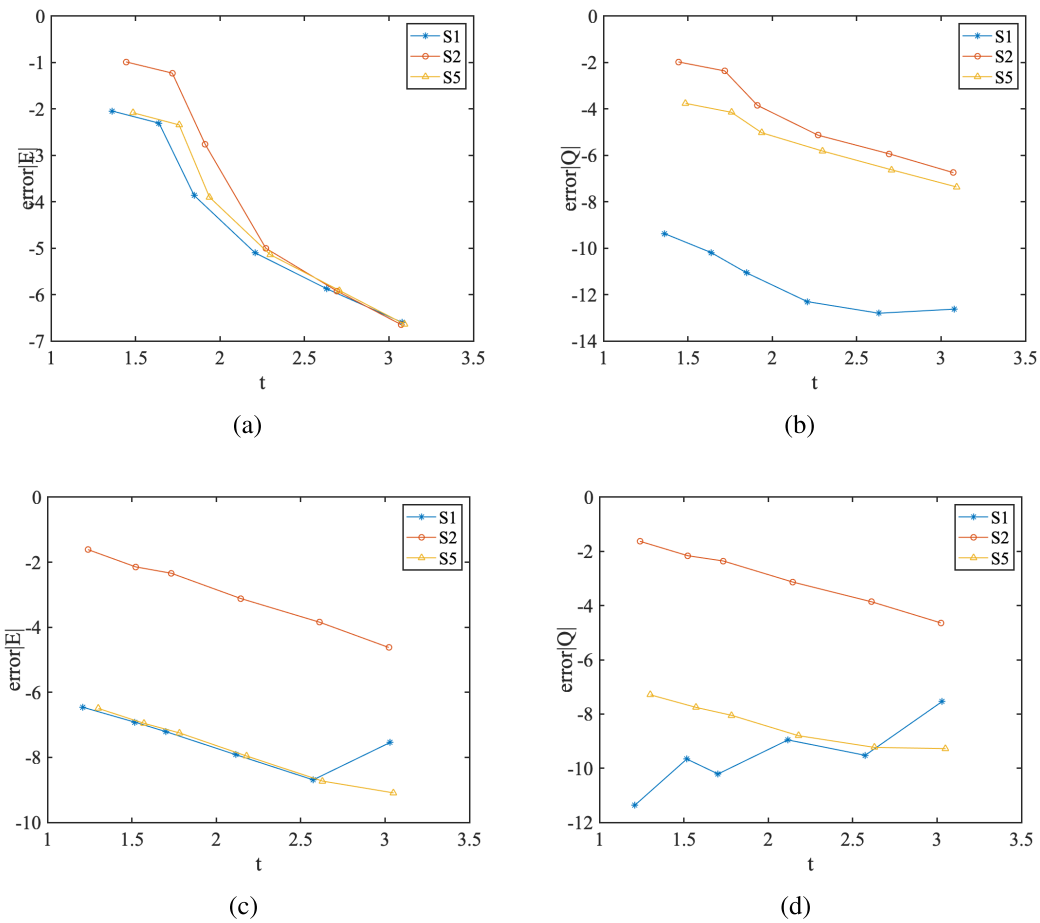

FIGURE 4. (a), (b): conserved quantities' approximations E, Q's errors of S1, S2 and S5 versus CPU times in bright solitons case; (c), (d): conserved quantities' approximations E, Q's errors of S1, S2 and S5 versus CPU times in dark solitons case.

7. CONCLUSIONS

The NLSE has four often-used discrete models: Model I, Model II, Model III, and Model IV, where Model I is a nonintegrable system, Modle II, Model III and Model IV are integrable systems. Numerical experiments demonstrate that Gauss method is more efficient than the nonsymplectic-nonsymmetric scheme and explicit symplectic schemes with same order, no matter applied to integrable models or nonintergrable model. Meanwhile, explicit symplectic schemes do not demonstrate their advantage of preserving structure. When using the same scheme for different models, for the conserved quantities' approximation FR_1, the results obtained in the nonintegrable Model I is significantly more efficient than those of the three integrable models. While for the conserved quantities' approximation FI_2, conclusion are just the reverse. Therefore, both intergrable models and nonintergrable model have their own advantages in preserving the conserved quantities' approximation of the original NLSE. For the three integrable models, Model II and Model III have similar simulation effect as the two models can be transformed by some simple transformation. For the integrable Model IV, because of complicated Doubarx transformations, it is diffcult to implement simulation, which leads to inefficiency. When using the error of Hamiltonian system's invariants as an indicator of simulation accuracy, symplectic schemes have the obvious advantage over the nonsymplectic-nonsymmetric schemes. In addition, symplectic scheme and symmetric scheme have very similar preservation of the invariants.

We also note here that, in sub-section 6.2 and 6.3, the indicator of simulation accuracy is the error of conserved quantities' approximation of the original NLSE, not that of invariants of the discrete Models. Therefore, the conclusions that we obtained is a slight different from the existing viewpoints about symplectic schemes' simulation.

Funding

This work was supported by the Fundamental Research Funds for the Central Universities (Nos. 2018ZY14, 2019ZY20 and 2015ZCQ-LY-01), Beijing Higher Education Young Elite Teacher Project (YETP0769) and the National Natural Science Foundation of China (Grant Nos. 61571002, 61179034 and 61370193).

REFERENCES

[1] M. J. Ablowitz, J. F. Ladik, Nonlinear differential difference equations and Fourier analysis, J. Math. Phys. 17 (1976) 1011–1018.
[2] R. E. Abraham, J. E. Marsden, Foundations of Mechanics, Benjamin-Cummings, Reading, MA, 1978.
[3] G. Acribis, Finite difference discretization of the cubic Schrödinger equation, IMA J. Numer. Anal. 13 (1993) 115-124.
[4] V. I. Arnold, Mathematical Methods of Classical Mechanics, Spring, New York, 1978.
[5] M. Delfour, M. Fortin, G. Payre, Finite-difference solutions of a non-linear Schrödinger equation, J. Comput. Phys. 44 (1981) 277-288.
[6] R. K. Dodd, J. C. Eibeck, J. D. Gibbon, H. C. Morris, Solitons and Nonlinear Wave Equation, Academic Press, 1982.
[7] A. M. Dunlop, E. M. Wright, W. J. Firth, Spatial soliton laser, Opt. Commun. 147 (1998) 393–401.
[8] H. Guan, Y. D. Jiao, J. Liu, Y. F. Tang, Explicit symplectic methods for the nonlinear Schrödinger equation, Commun. Comput. Phys. 6 (2009) 639–654.
[9] B.Y. Guo, The convergence of numerical method for nonlinear SchrSdinger equation, J. Comput. Math. 4 (1986) 121-130.
[10] E. Hairer, C. H. Lubich, G. Wanner, Geometric numerical integration, Springer, New York, 2002.
[11] B.M. Herbst, J.Ll. Morris, A.R. Mitchell, Numerical solution of the nonlinear SchrSdinger equation, J. Comput. Phys. 60 (1985) 282-305.
[12] A. Hasegawa, Optical Solitons in Fibers, Springer-Verlag, Berlin, 1989.
[13] V. V. Konotop, L. V*á*zquez, Nonlinear Random Waves, World Scientific, Singapore, 1994.
[14] G. L. Lamb, Elements of Soliton Theory, John Wiley & Sons, New York, 1980.
[15] J.M. Sanz-Serna, J.G. Verwer, Conservative and noneonservative schemes for the solution of the nonlinear Schriktinger equation, IMA J. Numer. Anal. 6 (1986) 25-42.
[16] J. M. Sanz-Serna, Methods for the numerical solution of the nonlinear Schrödinger equation, Math. Comput. 43 (1984) 21-27.
[17] G. Strang, On the construction and comparison of difference schemes, SIAM J. Numer. Anal. 5 (1968) 507–517.
[18] T.R. Taha, M. Ablowitz, Analytical and numerical aspects of certain nonlinear evolution equations. II. Numerical, nonlinear Schr'ddinger equation, J. Comp. Phys. 55 (1984), 203-230.
[19] Y. Tang, L. Vázquez, F. Zhang, V. M. Péerez-García, Symplectic methods for the nonlinear Schrödinger equation, Comput. Math. Appl. 32 (1996) 73–83.

[20] Y. Tang, V. M. Pérez-García, L. Vázquez, Symplectic methods for the Ablowitz–Ladik model, Appl. Math. Comput. 82 (1997) 17–38.

[21] Y. Tang, J. Cao, X. Liu, Y. Sun, Symplectic methods for Ablowitz–Ladik discrete nonlinear Schrödinger equation, J. Phys. A: Math. Theory 40 (2007) 2425–2437.

[22] Y. Tourigny, J. Morris, An investigation into the effect of product approximation in the numerical solution of the cubic nonlinear Schr'ddinger equation, J. Comput. Phys. 76 (1988) 103-130.

[23] Y. Yao, M. Xu, B. Zhu, Q. Feng, Symplectic schemes and symmetric schemes for nonlinear schrödinger equation in the case of dark solitons motion, Int. J. Model. Simul. Sci.Comput. 12 (2021) 2150056.

[24] V.E. Zakharov, A.B. Shabat, Interaction between solitions in a stable medium, Sov. Phys.-JETP 37 (1973) 823–828.

[25] F. Zhang, V. M. P*é*rez-Garcia and L. V*á*zquez, Numerical simulation of nonlinear Schr'ddinger systems: A new conservative scheme, AppL Math. Comput. 71 (1995) 165-177.

[26] R. Zhang, J. Huang, Y. Tang, L. Vazquez, Revertible and symplectic methods for the Ablowitz–Ladik discrete nonlinear Schrödinger equation, GCMS '11: Proceedings of the 2011 Grand Challenges on Modeling and Simulation Conference, pp. 297–306, 2011.

[27] B. Zhu, Y. Tang, R. Zhang, Symplectic simulation of dark solitons motion of nonlinear Schrödinger equation, Numer. Algor. 81 (2019) 1485–1503.

[28] B. Zhu, R. Zhang, Y. Tang, X. Tu, Y. Zhao, Splitting K-symplectic methods for noncanonical separable Hamiltonian problems, J. Comput. Phys. 322 (2016) 387–399.